AMSE JOURNALS –2014-Series: Modelling A; Vol. 87; N° 2; pp 89-108

Submitted Nov. 2013; Revised July 26, 2014; Accepted September 2, 2014

A New Approach Design Optimizer of Induction Motor using Particle Swarm Algorithm

S. Chekroun[1], B. Abdelhadi[2], A. Benoudjit[2],

[1] Research Laboratory on Electrical Engineering,
Faculty of Technology , M'Sila University, 28000, Algeria,
[2] Research Laboratory on the Electrical Engineering,
Faculty of Sciences Engineering, Batna University,
Rue Chahid M[d] El Hadi Boukhlouf, Batna – Algeria
(chekrounsalim1@yahoo.fr)

Abstract

First of all, this paper discusses the use of a novel approach optimization procedure to determine the design of three phase electrical motors. The new lies in combining a motor design program and employing a particle-swarm-optimization (PSO) technique to achieve the maximum of objective function such as the motor efficiency. A method for evaluating the efficiency of induction motor is tested and applied on 1.1 kW experimental machines; the aforementioned is called statistics method (SM) and based on the analysis of the influence losses. As the equations which calculate the iron losses make call to magnetic induction. From this point, the paper proposes to evaluate the B(H) characteristic by estimating the circuit's flux and the counting of excitation. Next, the optimal designs are analyzed and compared with results of another method which is genetic algorithms (GAs) optimisation technique, was done to demonstrate the validity of the proposed method.

Keywords: Particle Swarm Optimization (PSO), Efficiency Evaluation, Induction Motors.

1. Introduction

Recently, the induction motor comprises 95% of all motors utilized in machinery and the operating efficiencies of these machines greatly impact the overall energy consumption in industry. Current motors are produced with higher efficiency ratings than standard motors; But the decision to replace an existing motor focuses on the actual price savings that depend on several key points such as operating efficiency and the percentage of time at given loads, [1, 2].

In addition to the importance of induction motors, the aim of this paper is a contribution to energy saving efforts, specifically in the field of low power induction motors. This contribution is

kept in perspective by taking into consideration the energy saving potential during the motor design stage, as well as during its operation. The previous efforts were always made to save energy in motor application by using energy only as much as what was needed during operating. The best way is to exploit the saving potential during motor design. However, taking into consideration its intended application. It can be achieved either through the improvement of motor design or through the reduction of the electrical input energy when the motor has been already existed, [3].

Since, optimization techniques are strongly combined with the electrical motor design and stimulated by the pressure of demands in the motor market and its applications. The target is to get a design optimized which possess like the objective function minimum material cost, the minimum weight resulting in an optimum performance feature of the motor as maximum efficiency, [4, 5].

The optimization design of squirrel's cage induction motors is a complex nonlinear problem with constraints in the following aspects: At the beginning, there are too many variables involved in the problem and the many variables are combined with each other. So it is difficult to manipulate the spaces by small steps. After that, the problem has strong no convexity; and the property of the function will deteriorate when the rotor slots dimensions are optimized, etc. Therefore, this achievement is qualified at the local optimized solution resulting in the loss of the global one while parameters are optimized with a deterministic algorithm. During the development of the mathematics 'modem, many scholars introduced the random approach into optimization algorithm and advanced some new and powerful algorithmic models for non linear problems, [6, 7].

The PSO is recently proposed as a new optimization algorithm, [8]. The main idea is based on the food searching- behaviour of herd. It was observed that they take into consideration the global level of information to determine their direction. Therefore, the global and local best positions were counted at each instant of time (iteration). The output was the new direction of search. Once this direction is localized the cluster of birds follows it.

Finally, his paper is a sort of comparison between the loss reduction problem by the stochastic technique which is called particle swarm optimization (PSO) also, the genetic algorithm (AGs), [9].

2. Induction Motors' Efficiency

The efficiency can be expressed in terms of output power ($P_{Mechanical}$) and the sum of losses ($\sum Losses$), input power ($P_{Electrical}$), [1]:

$$\eta = \frac{P_{Mechanical}}{P_{Electrical}} = \frac{P_{Mechanical}}{P_{Mechanical} + \sum Losses} \tag{1}$$

To determine the efficiency several international standards existed. Basically, the difference between these standards lies in the additional load or stray-load losses are dealt with. Either a fixed

allowance is used, or by calculating the mechanical output power. The Japanese JEC 37 standard simply neglects the additional load losses. So, in the IEEE 112-B standard they are deduced by measuring the input and output power. However, the losses not covered which are by the 4 other loss terms: - the stator and rotor copper losses, the iron losses and the friction and windage losses. In the IEC 60034-2 standard, these losses are estimated at 0.5 % of the input power. The different ways of dealing with the additional load losses is the reason why efficiency values obtained from different testing standards can differ by several percent, [1, 2].

2.1 Motor Losses

There are four different kinds of losses occurring in induction motors which are the following: electrical losses, magnetic losses, mechanical losses and stray-load losses. Those losses can be counted:

2.1.a Iron losses

The calculation of iron losses makes it self by numerous methods as: a simplified method; magnetization rate analysis method or by analytical Method, [1, 10].

(a) Simplified Method

This method determines iron losses for the alternative supply when the magnetic performances of the materials are known, as clarified in, [11]. Several works [11, 12] propose the possibility of the iron losses separation in three parts:

1) Hysteresis Loss: Their contribution can be evaluated by this equation:

$$P_h = a\, f\, B_m^x \tag{2}$$

2) Supplementary losses: They are due to the variations Weiss domains losses when a variable magnetic field is applied to the magnetic materials. They are given by the following equation:

$$P_e = e\, f^{1.5}\, B_m^{1.5} \tag{3}$$

3) Classical losses: are the results of the eddy-currents' presence in all conductor materials. These losses are given by:

$$P_{ec} = b\, f^2 B_m^2 \tag{4}$$

Therefore, these currents become important by the presence of the skin effect. The most known relation to take into account the effect of this last is, [11]:

$$P_{ec} = b\, f^{1.5} B_m^2 \cdot \frac{\sinh(d.\sqrt{f}) - \sin(d \cdot \sqrt{f})}{\cosh(d \cdot \sqrt{f}) - \cos(d \cdot f)} \tag{5}$$

With B_m is the flux density, *a, x, e, b* and *d* are constants which vary according to the type and grad of the lamination material. Normally these are very difficult to determine analytically and empirically values or test measurements are used (ex. Epstein's frame).

Then, in general case where the power supply is alternative non sinusoidal the equation (6) is adopted for the iron losses prediction [12, 13]:

$$P_{fer} = \alpha \cdot V_{moy}^{x} + \beta \cdot V_{eff}^{2} \tag{6}$$

With, V_{moy}, V_{eff} are respectively a middle and rms voltage, x is a Steinmetz coefficient and α, β are a coefficients.

(b) Magnetisation Rate Analysis Method

The assessment is based on the integration of the losses due to the two phenomena which intervene in magnetization time; the losses by movement of the domains and the losses by the rotation of the magnetic moments. Experimentally, the value of these losses can be deducted by the flux density rate. This methodology is adopted with the ferromagnetic model [13].

The tests' standard, used the Epstein frame to give the satisfactory results for a sinusoidal flux density. But the losses correspond to a sum of flux densities and frequencies during the tests. This method did not provide us with any information on the variation of the losses by Hysteresis. A new approach for the losses measure has been developed to complete the Epstein method. This method gives the possibility to determine the magnetic losses for a shape of any flux density by integration of the value of the losses during a cycle.

$$P_T = f \cdot \int_0^T P_d \cdot (r_m \cdot B)\, dt \tag{7}$$

Hence, P_T are the total losses, P_d power absorbed during the magnetization, r_m is the magnetization rate, B is instantaneous flux density and T a period.

(c) Analytic Method

For an alternative field the losses are expressed in the following form:

$$P_{fe} = C_H \, f \, \hat{B}^{\alpha} + C_E \cdot (\omega_s \, \hat{B})^2 \tag{8}$$

Where C_H , α and C_E are constants that vary according to the type and the grad of lamination material obtained experimentally by Epstein frame. f is the frequency of the supply and $\hat{B}$ is the peak flux density calculated from the flux.

The harmonics effects are taken into account by the use of conventional method though modifying the loss coefficients. The Hysteresis loss P_{FeH} and the eddy-current loss P_{FeE} are calculated according to the following equations, [5]:

$$\left.\begin{aligned} P_{ferH} &= \int_{Va} [\sum_{n=1}^{n} C_{Hn}(nf_s) \cdot B_n^2]\, dv \\ P_{ferE} &= \int_{Va} [\sum_{n=1}^{n} C_{En}(nf_s)^2 \cdot B_n^2]\, dv \end{aligned}\right\} \tag{9}$$

Where V_a is the core volume. However, C_{Hn} and C_{En} are the Hysteresis and eddy-current loss coefficients associated with n^{th} harmonic, $B_n(x,y)$ is the flux density amplitude, [14].

Mr. Kytomaki elaborated a comparative study between the conventional method and the finite-elements models. He declared :<< Because of the uncertainties in the iron loss calculation methods. A new statistical method has been introduced. This last utilizes a construction data and analytically calculated magnetic field values. The iron losses are defined by nine design factors >>.

$$P_{fer} = 10^{\begin{bmatrix} C_0 + C_1 B_\delta + C_2 m_{fer,Z1} + C_3 2p + C_4 q + C_5 b_{11} + \\ C_6 B_{1r} + C_7 f + C_8 K_K + C_9 Q_2 \end{bmatrix}} \quad (10)$$

Where $C_0 \ldots . C_9$ are coefficients given by [11], $m_{fe,Z1}$ is the mass of the teeth and the details have been presented by Crank - Nicholson [6, 10].

2.1.b Stray-load losses

These losses are very difficult to model and to quantify. Although, the stray-load losses were the theme of several studies and analysis, the phenomena that govern these losses are still under discussion, particularly from the measurement point of view. The standard IEEE 112-B defines these losses as the difference between the total measured losses and the conventional losses, [2, 14]. In order to, minimize these losses several solutions are proposed in literature like the rotor bar insulation which is used to limit the inter-bars leakage currents, Or by using a double layer winding with low space harmonic contribution. In addition to that, a reductions flux variations in the motor teeth for high frequency.

2.1.c Copper losses

The third component of losses is ohmic heading. The last is determined by a number of stator and rotor joule losses. The first are evaluated using the winding resistance measured in direct current and reported at the reference temperature. It depends on the machine insulation class. For this reason, it is independent by the real temperature reached during the load tests. As an example, for insulation class F an over temperature of 115°C has to be considered. The rotor joule losses are evaluated as the product of the rotor slip and the air gap transmitted power.

Consequently, copper losses have negative effects on the motor efficiency. Hence, it is necessary to minimize these losses. For example, using conductors of large diameters in order to reduce the resistance per unit length of the conducting windings, [1, 10].

2.2 Energy Efficient Motor

The vast majority motor manufacturers had provided a special category of product with increased efficiency and evidently higher price. However, questions arised about the application of energy efficient motors. Users of major industrial companies are frequently faced to the decision of buying more expensive motors; But with a feeling of uncertainty about the presumed

economical advantages. It must be emphasised that a number of factors which may affect the motor efficiency include: power' supply quality, careful attention to harmonics, mechanical transmission and maintenance practices, [1, 4].

Since, induction motors are the most commonly employed electrical machines in industry throughout the world today. Consequently, investment in the quality of motor that enables a reduction of its losses. Although, a small percent that is frequently neglected is usually a financial sound practice.

This paper describes the use of a formal optimisation procedure to determine the design of an induction motor to obtain maximum efficiency. The method involved the use of a design process coupled to an optimisation technique such as, the PSO.

3. Optimization Techniques

Recently, research efforts have been made in order to invent now optimization techniques for solving daily life problems which had the attributes of memory update and population-based search solutions. General-purpose optimization techniques as an example, Particle Swarm and Genetic Algorithms, had become standard optimization techniques which principal are:

3.1 Genetic Algorithms (GAs)

Genetic Algorithms are research methods that employ processes found in natural biological evolution. These algorithms search or operate on a given population of potential solutions to find those that approach some specification or criteria. To reach the aim, the algorithm applies the principle of survival of the fittest to find better approximations. At each generation a new set of approximations are created by the process of selecting individual potential solutions (individuals) according to their level of fitness. The domain's problem breed them together using operators borrowed from natural genetics. This process leads to the evolution of population of individuals that are better suited to their environment than the individuals that they were created from natural adaptation, [4, 5].

Generally, the GAs will include the three fundamental genetic operations of selection, crossover and mutation. These operations are used to modify the chosen solutions and select the most appropriate offspring to pass on to succeeding generations. GAs considers many points in the research space at the same time it provides a rapid convergence to a near optimum solution in many types of problems. In other words, they usually exhibit a reduced chance of converging to local minima. GAs suffers from the problem of excessive complexity if used on problems that are too large, [7].

3.2 Particle Swarm (PS)

From a view of social cognition, each individual in PS can benefit from both its own experience and group findings. In its theoretical base some factors are included, [7, 8 and 9]:

- Evaluation of stimulation; - Influence to its behavior hereafter by its own experience;
- Influence to its behavior by other particles' experience.

The principle of PSO algorithm is as follows, [7]. Let X and V denote the particle's position and its corresponding velocity in research space respectively. Therefore, the i^{th} particle is represented as:

$$X_i = (x_{i1}, x_{i2}, \ldots x_{iD}), i = 1,2,\ldots m \tag{11}$$

In the D-dimensional space the best previous position of the i^{th} particle is recorded and represented as:

$$P_{besti} = (p_{i1}, p_{i2}, \ldots p_{iD}), i = 1,2,\ldots m \tag{12}$$

The best one among all the particles in the population is represented as:

$$P_{gbest} = (p_{g1}, p_{g2}, \ldots p_{gD}), i = 1,2,\ldots m \tag{13}$$

The velocity of particle is represented as:

$$V_i = (V_{i1}, V_{i2}, \ldots V_{iD}) \tag{14}$$

Each particle of the population modified its position and velocity according to the following formulas:

$$v_{id}^{t+1} = w.v_{id}^{t} + C_1.rand.(p_{id} - x_{id}^{t}) + C_2.Rand.(P_{gd} - x_{id}^{t}) \tag{15}$$

$$x_{id}^{t+1} = x_{id}^{t} + v_{id}^{t+1} \tag{16}$$

Where $d= 1, 2,\ldots D$ is one of the particles, $i=1,2,\ldots m$ is the number of particles in a swarm, x_{id}^{t} is position of particle in a single dimension and v_{id}^{t} velocity magnitudes are clipped to a predetermined $[-v_{min}, v_{max}]$ at the moment t, C_1, C_2 are acceleration constants; *rand* are random numbers distributed between [0, 1], w is an inertia weight introduced to improve PSO performance:

$$w = w_{max} - \frac{w_{max} - w_{min}}{d_{max}} \cdot d \tag{17}$$

4. Improving Efficiency Description by PSO Techniques

The following Fig.1 depicts the induction motor design optimization with PSO algorithm and includes two phases. The first phase represents the exploitation of a general design program, a series of alternative design for the specified power, to give the best geometrical model. Once, the machine is already achieved. In the second phase, we apply the optimization phase for the efficiency improvement, [15, 16].

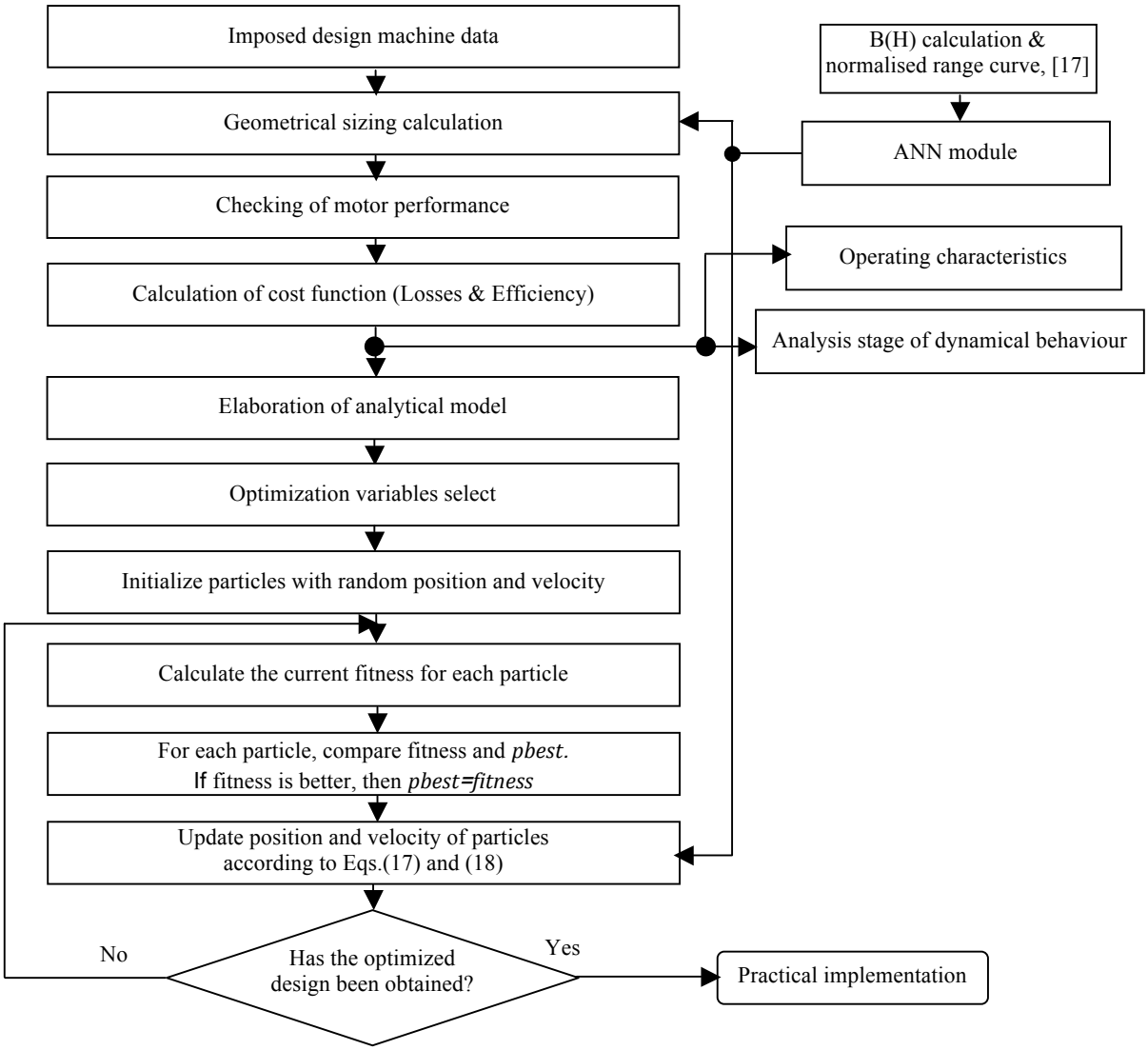

Fig. 1 Global flowchart of induction motor optimization process

4.1 Analytical Model

The design procedure of electrical machine is based on Liwschitz method which can be summarized in two main stages:

- From the imposed machine design data within Artificial Neural Network (ANN) interpolation of the normalized range curves. The type of ANN that we simulated is a multilayered network. Therefore, we use back propagation algorithm for its training. The in proposed method of optimization process which we intend to do is saturation test phase so that we can study the performances of the ANN and accomplish the task of the optimization. The entries are the B(H), saturation and form factors, which means that the number of entries of this network is equal to 4. Finding the optimized dimensions, which characterized by the active volume given by the inner stator diameter and the core length of the machine. However, this lead to the parameters of the electrical equivalent circuit of the machine and the current circular diagram, [18, 19];
- From the results of stage 1 evaluating the machine performances in order to check or not the machine analytical model.

(a) B(H) Curve Determination

Several methods are proposed for the determination of B(H) characteristic as:

-With two coils test; - One coil (with or without sensor) test.

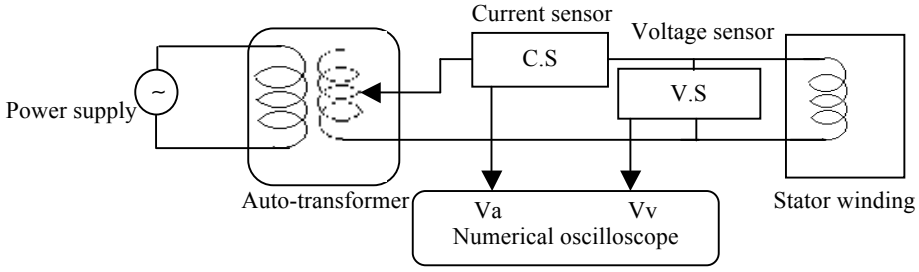

Fig. 2 Experimental setup

For this, in our case where access to the machine is possible through the stator. Then the latter proposes to use the test with a coil sensor in Fig. 2 such as, the test was performed on a rotating machine. The passage at the characteristic B(H)*)* makes itself through the following operations:

$$\phi_{max} = \frac{\frac{Vv}{2} Gv}{N_1 \cdot 314} \tag{18}$$

$$B_{max} = \frac{\phi_{max}}{S_{z1}} \tag{19}$$

$$I_{max} = \frac{Va}{2} Gi \tag{20}$$

$$H_{max} = \frac{N_1 \cdot I_{1max}}{L} \tag{21}$$

Where ϕ_{max} is maximal flux, Vv and Va are the two sensor outputs, Gv, Gi sensor gains given by the manufacturer, H_{max}, I_{1max} field density and current maximal, B_{max} flux density, and S_{z1} is a section of the stator teeth, [20].

This procedure is applied on a induction motor type DIN-IEC –F [AMSE, 19] considering some constraints in terms of voltage, number of poles, speed range, and its necessary data specifications as 1.1 kW, 220V, 0.74%, 1400 trs/mn.

The geometric sizes of the studied machine are necessary for the approach of the magnetisation curve. They are carried in the Fig. 3 and in agreement with the finite element method.

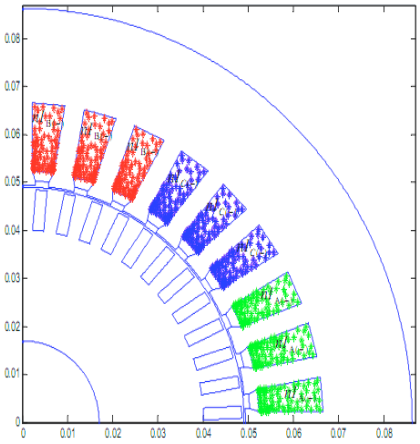

Fig. 3 Sketch of a pole of studied motor

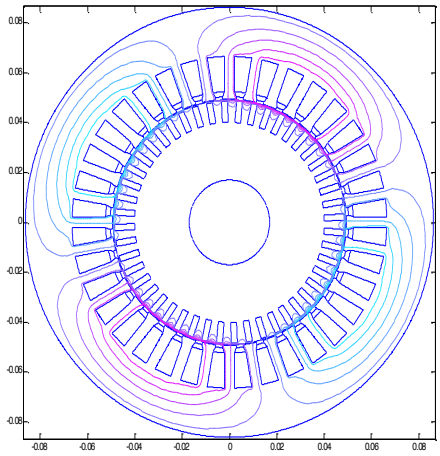

Fig. 4 Field lines middle course configuration

By substituting (18) in (19) then, (20) in equation (21) the B(H) figure obtained from the laboratory as shown in Fig. 5 compared with standard curve, [17].

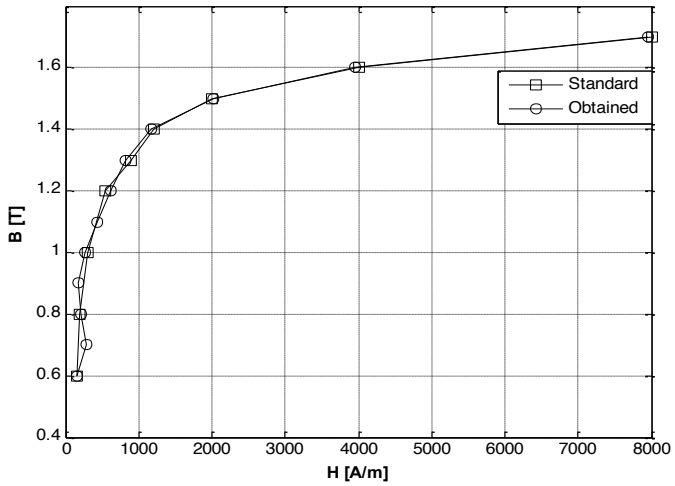

Fig. 5 Experimental B(H) curve

(b) Computed Design Results

The use of an experimental B(H) curve and the statistics method. The numerical investigation results which has been obtained from the design interface developed in our group for classical induction machines' design under MATLAB environments are reported in Table 2.

Table 2. Induction motor non-optimized calculated parameters for an experimental B(H) curve

Motor parameters	**Value**
Stator phase current $I_s\,(A)$	2.781
Air-gap length $\delta\,(mm)$	0.3
Peak air-gap flux density $B_\delta\,(T)$	0.641
Inner stator diameter $D\,(mm)$	114.59
Stator turns per phase N_1	378
Stator back iron thickness $h_{j1}(mm)$	18.0
Stator slot height $h_{t1}(mm)$	12.63
Stator slot / Rotor bar number	36/48
Stator back iron flux density $B_{hj1}(T)$	1.30
Tooth flux dens in stator $B_{t1}(T)$	1.446
Rotor back iron flux density $B_{hj2}(T)$	0.57
Rotor tooth flux density $B_{t2}(T)$	1.48
Mutual inductance $M\,(H)$	0.79214
Rotor resistance referred to the stator side $R_r'\,(\Omega)$	7.4426
rotor leakage reactance referred to the stator side $l_{\sigma r}'\,(H)$	0.02374
Stator phase resistance $R_s\,(\Omega)$	7.80
Total reactance $X_{\sigma tot}\,(\Omega)$	16.230
Total resistance $R_{\sigma tot}\,(\Omega)$	15.4845
Stator leakage reactance $X_{\sigma 1}\,(\Omega)$	8.0797
Starting current I_{1cc}(A)	10.126
Phase angle at the short-circuit $\varphi_{cc}\,(rd)$	0.8089
Stator phase r.m.s current at no-load (I_o)	0.862
Phase angle at no-load $\varphi_0\,(rd)$	1.4507
Efficiency $\eta\,(\%)$	75.9
------- $T_{star}\,/\,T_n$	1.84
Motor total weight W_{tm}(kG)	13.756

As a result of this investigation, the two points (a_0) and (a_{cc}) of the current circular diagram Fig.6.

$$a_0 \equiv \left(I_0 \cdot \sin\varphi_0 \;\; ; \; I_0 \cdot \cos\varphi_0\right) \tag{22}$$

$$a_{cc} \equiv \left(I_{1cc} \cdot \sin\varphi_{cc} \;\; ; I_{1cc} \cdot \cos\varphi_{cc}\right) \tag{23}$$

Where, the stator no-load current (I_o) comprises the magnetizing current (I_{m_o}) and loads losses one.

$$I_0 = I_{m0} + I_{oa} \tag{24}$$

In addition to the starting current I_{1cc} which is calculated from the equation (25):

$$I_{1cc} = \frac{V_1 \cdot (1 + \sigma_{H1})}{\sqrt{(X_{\sigma tot})^2 + (R_{\sigma tot})^2}} \tag{25}$$

$$X_{\sigma tot} = X_{\sigma 1} + \left[(1 + \sigma_{H1}) \cdot X'_{\sigma 2} \right] \tag{26}$$

$$R_{\sigma tot} = R_1 + \left[(1 + \sigma_{H1}) \cdot R'_2 \right] \tag{27}$$

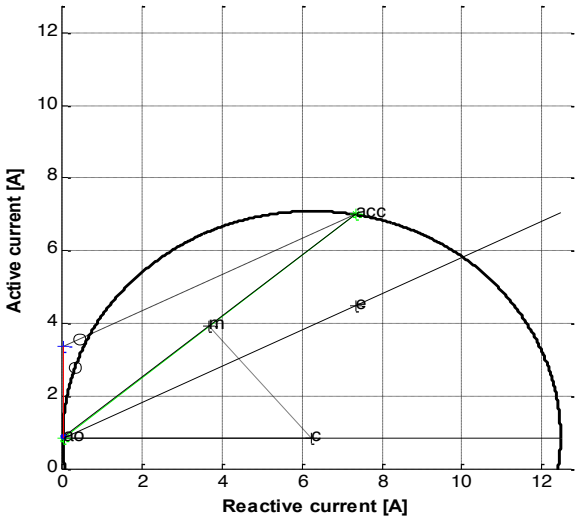

Fig. 6 Current circular diagram with computer aided design

The presented study is completed by another subprogram for simulation purpose of conceived motors. Fig. 7 to 12 presents the main characteristics of these motor.

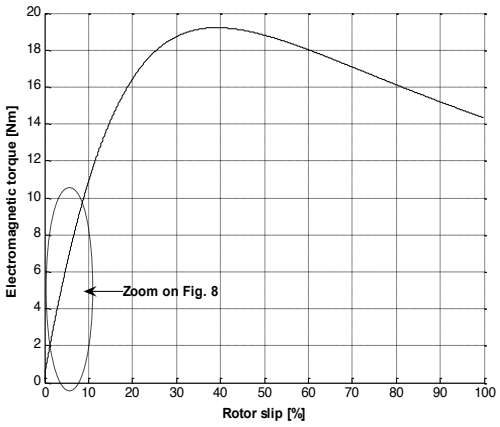

Fig. 7 Electromagnetic torque versus slip

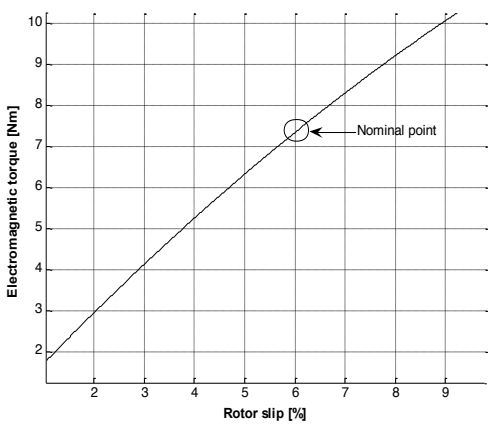

Fig. 8 Zoom ed region electromagnetic torque versus slip

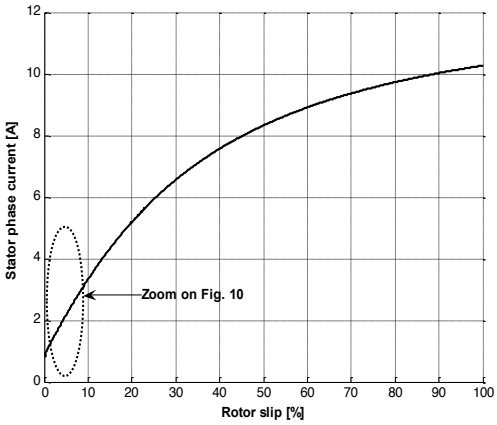

Fig. 9 Stator phase current versus slip

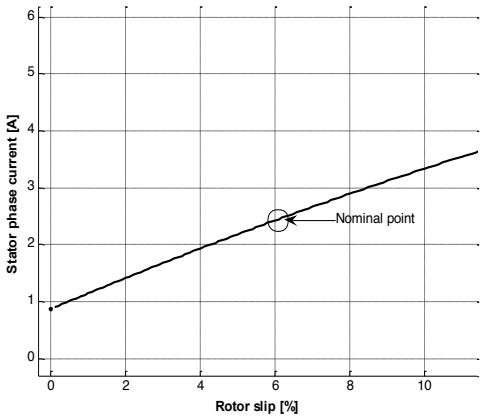

Fig. 10 Zoom ed region stator phase current versus slip

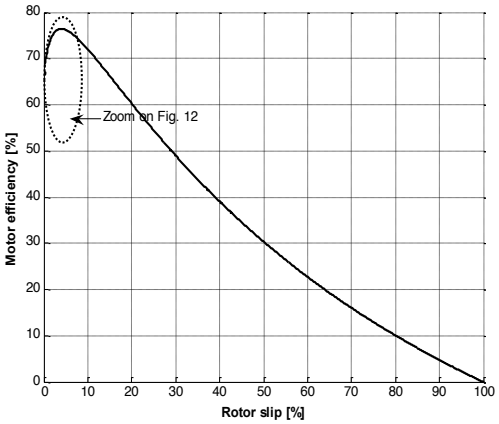

Fig. 11 Motor efficiency versus slip

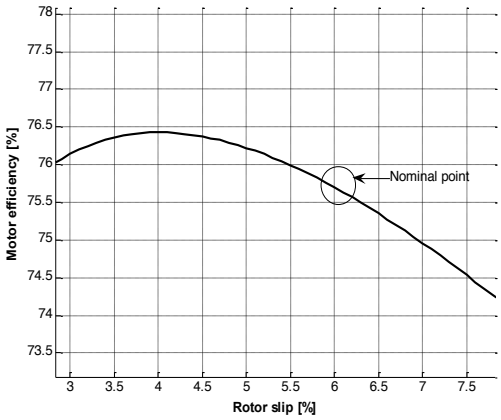

Fig. 12 Zoom ed region motor efficiency versus slip

(c) Dynamical Models and Performances Analysis

The dynamic performance of an AC machine is some how complex due to the coupling effect between the stator and rotor parameters which vary with rotor position. This can be simplified by using the d-q axis theory; as a result the time- varying parameters are eliminated. The dynamical model of induction machine used is represented by a fourth order state space model for the electric part and by a second order system for the mechanical part of the machine. Meanwhile the electrical variables and parameters are given in Table 2.

The simulation analysis of these three-induction motor was performed using SIMULINK blocks and power system blocks within SIMULINK toolbox under MATLAB environment. Within the block diagrams the induction motor is represented by the according block which models electric and mechanical dynamics and the three phase sources.

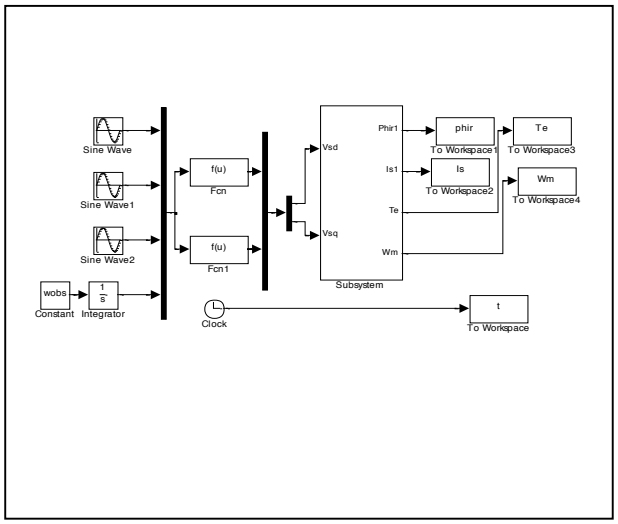

Fig. 13 Block diagram of performances analysis

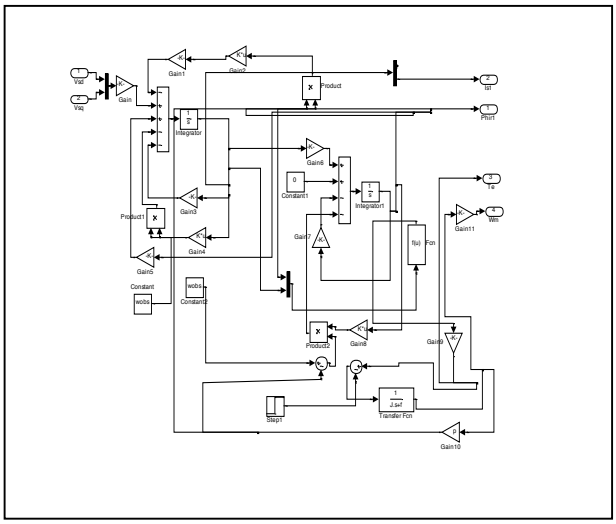

Fig. 14 Sub-system block

In the first test, the machine will be fed during three phase source Fig. 13 to simulate the starting phase of the motor under full load conditions ($Tl = 7.5Nm$). It can be seen from Figures 15 and 16, that the ($\hat{Is} = 3.82A$) and the rotor speed is ($nr = 1400\,trs/mn$).

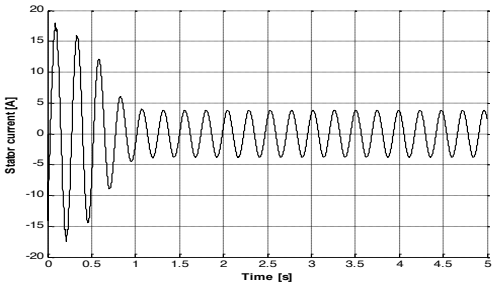

Fig. 15 Stator current versus time

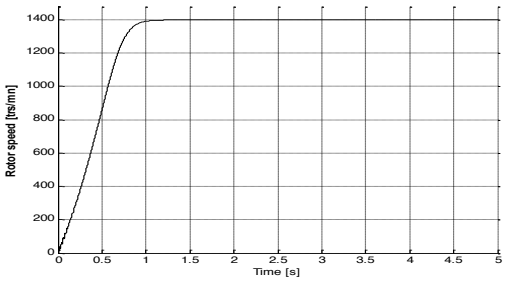

Fig. 16 Rotor speed versus time

In the second test, by varying the loads in order to analyze the starting torque value. Fig. 17 illustrates this hard condition ($T_l = 14.1Nm$). Then, after 2 seconds the load torque is stepped to the maximum values in order to check the pull-out torque. It can be seen from Figures 18, 19 and 20 that ($T_{l\,max} = 19Nm, Is_{max} = 10.25A$).

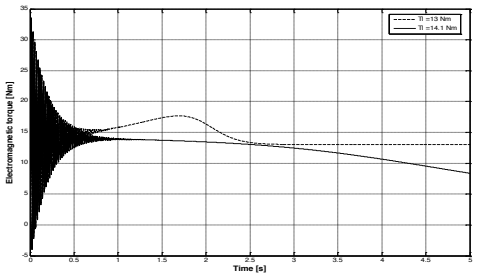

Fig. 17 Electromagnetic torque versus time

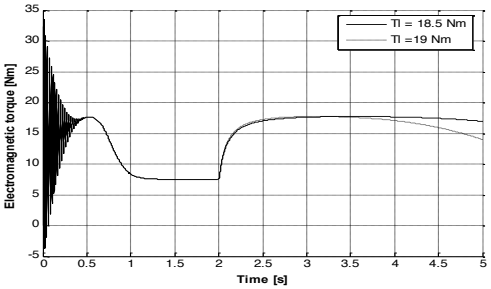

Fig. 18 Electromagnetic torque versus time

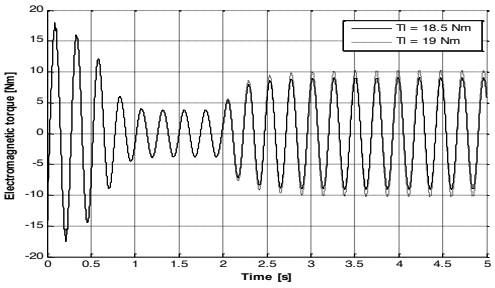

Fig. 19 Stator current versus time

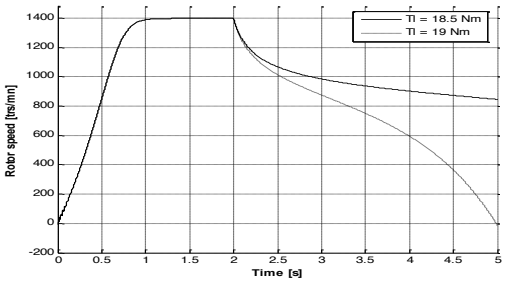

Fig. 20 Rotor speed versus time

Table 3 presents and compares the main performances of these motor, where it can be concluded that the analytical model is in good correlation and it can be accepted for optimization phase.

Table 3. Induction motor performances comparison

Motor parameters	**Statically analyzed**	**Dynamical analyzed**	**Data base**
Stator phase current $I_s(A)$	2.781	2.709	2.78
Starting current I_{1cc} (A)	10.23	10.25	10.72
Slip S(%)	6.5	6.66	6.67
Efficiency η (%)	75.9	---------	74
Rated T_{star}/T_n	1.84	1.88	2.1
Rated T_{max}/T_n	2.49	2.53	2.3
Motor total weight W_{tm} (kG)	13.756	---------	12

4.2 Optimization Phase

In order to obtain an acceptable design, Table 4 summarized the practical domains for the design parameters. Within case presented here, eight design parameters some of which are used in literature and affect induction motor's first order basic geometry is chosen. So, the efficiency (motor losses) is selected as main objective function and the weight of motor is selected as a constraint of optimization.

Table 4. Design variables and their limit values

variables	**Search region**
Inner stator diameter (mm)	$114 \le D \le 118$
Geometric report	$0.75 \le \lambda \le 1$
Stator slot height (mm)	$10 \le h_{t1} \le 14$
Back iron thickness (mm)	$14 \le h_{j1} \le 18$
Air-gap length (mm)	$0.3 \le \delta \le 0.5$
Stator tooth flux density (T)	$1.3 \le B_{t1} \le 1.7$
Rotor tooth flux density (T)	$1.4 \le B_{t2} \le 1.8$
Machine weight (kG)	$10 \le M \le 15$

We simulate the receding optimization of the objective function. PSO learning factors $c_1 = c_2 = 2,\ w_{max} = 0.95\ w_{min} = 0.4, iter_{max} = 50, pop_{size} = 30$

Table 5 shows and compares the values for the eight design parameters of the PSO with those GAs techniques. Accordingly, the PSO algorithm has returned an acceptable solution which is indicated by a good value for the objective with no constraint violation.

Table 5. Design parameter values obtained after optimization

Parameters	Solutions with PSO technique	Solutions with GAs method
Inner stator diameter (mm)	115.57	114.6
Geometric report	0.9653	0.9316
Stator slot height (mm)	10.49	11.9
Back iron thickness (mm)	14.16	15.9
Air-gap length (mm)	0.4457	0.5
Stator tooth flux density (T)	1.469	1.55
Rotor tooth flux density (T)	1.523	1.65
Machine weight (kG)	13.002	12.69
Optimized efficiency (η_{Opt} %)	78.06	77.92

Fig. 21 and 22 show graphs corresponding to the progress of each algorithm for 30 populations of each variable.

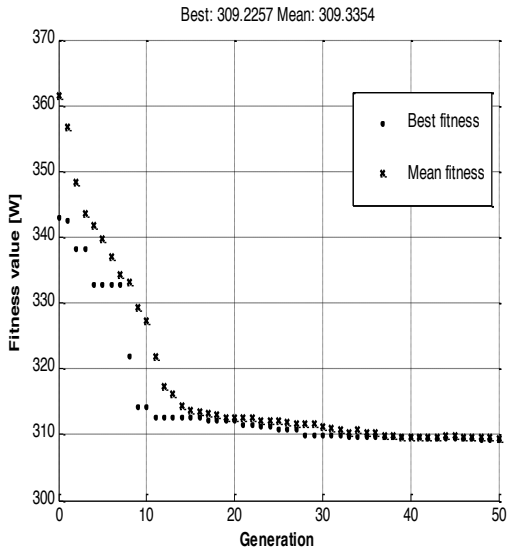

Fig. 21 Evolution of PS average and best fitness functions

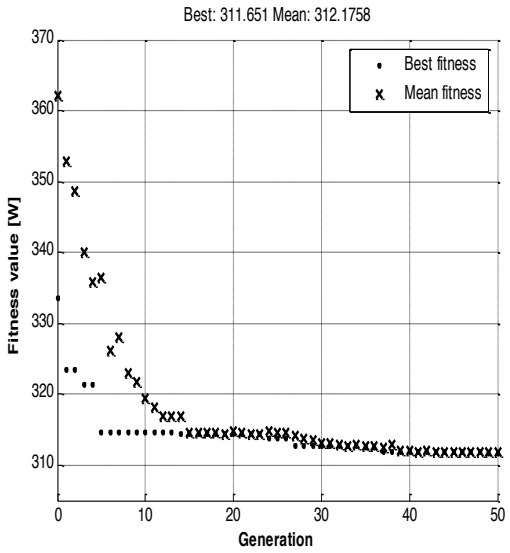

Fig. 22 Evolution of GAs average and best fitness functions

Fig. 21 illustrates the fitness function variation with the generation numbers during the optimization process. With eight particles in each generation the PSO converges to its optimum with sufficiently small error within *15* generations (error is 0.2*)*.

Fig. 22 depicts the mean and best individuals versus generation number for optimization machine by GAs. It can be noted that the highest efficiency value (77.92%) is reached for a minimum fitness function representing the motor losses at the 15th generations and the results of the best-yielded machine which reported in Table 6 and Fig. 23 to 26. The latter, depict examples of performance characteristics of standard and optimum design.

Table 6. Comparison of the data base and simulation results

Motor parameters	**Calculated motor**	**Optimizing motor**	
		PSO	**GAs**
Starting current I_{Icc} (A)	10.23	11.58	11.12
At no load	0.85	1.69	1.63
Nominal current	2.781	3.127	3.002
Efficiency η (%)	75.9	78.06	77.62
Rated T_{star} / T_n	13.8 / 7.5	16.31 / 8.11	15.82 / 8.11
Rated T_{max} / T_n	18.67 / 7.5	21.85 / 8.36	21.19 / 8.11
Motor total weight W_{tm} (kG)	13.756	13.002	12.69

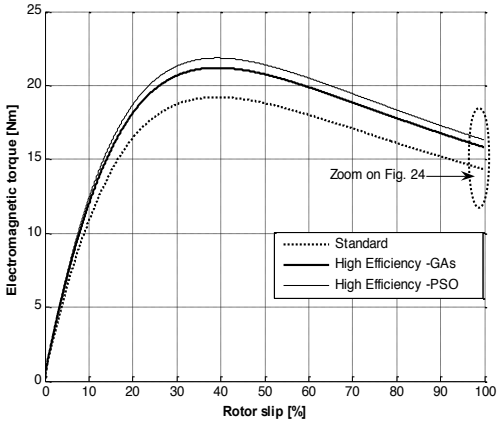

Fig. 23 Electromagnetic torque versus slip

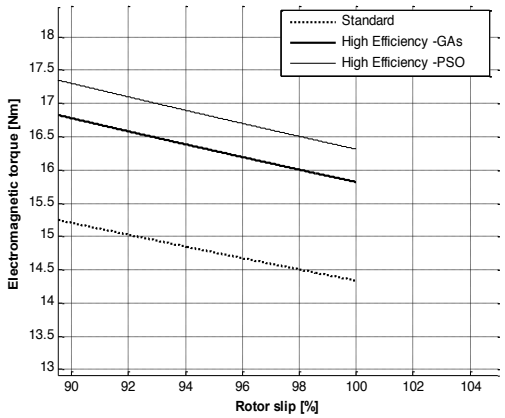

Fig. 24 Zoom ed region electromagnetic torque versus slip

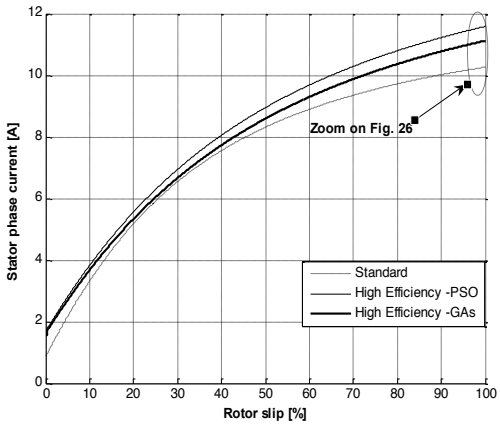

Fig. 25 Stator phase current versus slip

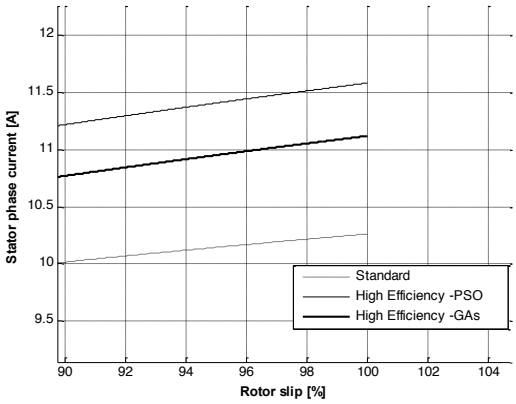

Fig. 26 Zoom ed region stator phase current versus slip

According to obtained results, while achieving performance improvements, the efficiency of the motor is increased by about (2%). This difference correspond to approximately (22 W) at full load which is important. From one point, starting torque and pullout are desirably increased ($\approx 2Nm$). From the other point, a small decrease in motor total weight is observed from the results. Therefore, it can be said that PSO is suitable for motor design and can reach successful designs with lower weight, higher torque, and higher efficiency than the standard motor meanwhile satisfying almost every constraint.

Relying on what has been mentioned before. There are other studies which already dealt with this field of study by relying on another method (AGs), [21]. However, our study can be considered as a current good direction.

5. Conclusion

Finally, this paper has presented the results of particle swarm optimization algorithm and a new application of it for solving the induction motor design problem, obtained from the machine design program developed in our laboratory.

In order to validate the conceived motor, a series of simulation and analysis test through MATLAB simulations were performed. These techniques were found very valuable, mainly for costly systems before optimization technique. In fact, results on a machine type DIN-IEC –F system demonstrate the feasibility and effectiveness of the proposed method, and the comparison at AGs technique shows its validity.

6. References

1. A. Boglietti, A. Cavagnino, M. Lazzari, and M. Pastorelli, "Induction Motor Efficiency Measurements in Accordance to IEEE 112-B, IEC 34-2 and JEC 37 international standards," *Conference Proceedings on Electric Machines and Drives,* Madison, WI, USA, Vol. 3, pp. 1599-1605, 1- 4 June, 2003.
2. D. JunKim, J. Choi, Y. Chun, and Dae-Hyun Koo and Pil-Wan Han†, ''The Study of the Stray Load Loss and Mechanical Loss of Three Phase Induction Motor considering Experimental Results,'' *J Electr Eng Technol*, Vol. 8, pp. 742-747, 2013.
3. C. Thangaraj, S. P. Srivastava, and Pramod Agarwal, '' Particle Swarm Optimized Design of Poly-Phase Induction Motor with the Consideration of Unbalanced Supply Voltages, '' *Int. Journal of Mathematical Modeling, Simulation and Applications*, Vol. 1, N^{o}. 3, pp. 339-350, 2008.

4. L. Vuichard, P. Schouwey, M. Lakhal, M. Ghribi et A.Kaddouri, ‘‘Optimisation Energétique par Logique Floue dans un Moteur à Induction Triphasé,” *Canadian Conference on Electrical and Computer Engineering*, pp. 1082 - 1085, May, 2006.
5. S. Sivaraju, N. Devarajan, “Novel Design of Three Phase Induction Motor Enhancing Efficiency, Maximizing Power Factor and Minimizing Losses” *European Journal of Scientific Research*, Vol. 58, N°. 3, pp. 423-432, 2011.
6. C. Singh, D. Sarkar, “Practical Considerations in the Optimisation of Induction Motor Design,” *Electric Power Applications*, Vol. 139, N°. 4, pp. 365 - 373, July, 1992.
7. A. Raghuram, V. Shashikala, ‘’Design and Optimization of Three Phase Induction Motor Using Genetic Algorithm,” *International Journal of Advances in Computer Science and Technology,* Vol. 2, N°. 6, pp. 70-76, June, 2013.
8. H. Jang, C. Hwan and C. Gyun, ‘Particle Swarm Optimisation Based Optimal Power Flow for Units with Non-Smooth Fuel Cost Functions," *AMSE. Journal*, *Modelling*. A, Vol. 83, N°.3, 2010.
9. R.H.A. Hamid, A.M.A. Amin and R.S. Ahmed,’’ New Technique for Maximum Efficiency and Minimum Operating Cost of Induction Motors Based on Particle Swarm Optimization (PSO),’’*IEEE Industrial Electronics*, Vol. 6, N° 10, pp. 1029-1034, Nov, 2006,
10. G. Grellet, ‘‘Pertes dans les Machines Tournantes’’, Technique de l’Ingénieur, D3450, Décembre, 1989.
11. Boglietti, A. Cavagnino, "Two Simplified Methods for the Iron Losses Prediction in Soft Magnetic Materials Supplied by PWM Inverter", *4th International Symposium on Advanced Electromechanical Motion System*, Bologna, Italy, 19-20 June, 2001.
12. A. Boglietti, M. Lazzari, ‘‘A Simplified Method for the Iron Losses Prediction in Soft Magnetic Materials with Arbitrary Voltage Supply’’, *4th International Symposium on Advanced Electromechanical Motion System*, Bologna, Italy, 19-20 June, 2001.
13. M. S. Lancarotte, G.Arruda, ‘‘Estimation of Core Losses Under Sinusoidal or Non-Sinusoidal Induction by Analysis of Magnetization Rate’’, *4th International Symposium on Advanced Electromechanical Motion System*, Bologna, Italy,19-20, June, 2001.
14. R. Kytomaki, A. Arkkio, ‘‘Validity of Conventional and Modern Methods of No-Load Loss Calculation in Asynchronous Machines Statistic Approach’’, *IEE Conference Publication* N°.44, 1997.

15. J. A. Moses, J.L. Kirtley, “A Computer-Based Design Assistant for Induction Motors,” *IEEE. Industry Applications Society Annual Meeting Conference Proceedings,* Vol. 1, pp. 1 - 7, 28 September-4 October, 1991.
16. F. You-tong, F. Cheg-zhi, "Application of stochastic Method to Optimum Design of Energy-Efficient Induction Motors With a Target of LCC", *Journal of Zhejiang University Science*, Vol. 4, N°. 3, May-June, 2003, pp. 270-275.
17. M. Liwschitz et L. Maret "Calcul des Machines Electriques", Tome 1, Tome 2, Edition Dunod, Paris, France, 1967.
18. S. Chekroun, B. Abdelhadi and A. Benoudjit, «Design Optimization of Induction Motor Efficiency by Genetic Algorithms," *AMSE Journal*, Modelling. A, Vol. 81, N°.2, pp. 14-29, January/February, 2009.
19. T. Hiyama, M. Ikeda, and T. Nakayama, ‘‘Artificial Neural Network Based Induction Motor Design,” *Power Engineering Society Winter Meeting*, Vol. 1, pp. 264-268, August, 2002.
20. M. Gerl, J. Paul Issi, ‘‘Physique des Matériaux’’, *Presses Polytechniques et Universitaires Romandes*, Vol. 8, 1996.
21. M. Çunka and R. Akkaya, “Design Optimization of Induction Motor by Genetic Algorithm and Comparison with Existing Motor,” *Math. Comp. Applications,* Vol. 11, N°. 3, pp. 193-203, 2006.